ELSEVIER

Inorganica Chimica Acta 227 (1994) 91–97

Inorganica Chimica Acta

Spectroscopic studies of the *trans*-$[VOCl_2(H_2O)_2]$ chromophore in its hydrogen bonding adduct with 18-crown-6

Nagao Azuma *, Takehiro Ozawa

Department of Chemistry, Faculty of General Education, Ehime University, Matsuyama 790, Japan

Received 17 February 1994; revised 23 May 1994

Abstract

An electron paramagnetic resonance (EPR) study has been carried out on a single crystal of *trans*-$[VOCl_2(H_2O)_2](18\text{-crown-6})\cdot 2H_2O$ or adduct of *trans*-diaquadichlorooxovanadium(IV) with 1,4,7,10,13,16-hexaoxacyclooctadecane (abbr. 18C6) at ambient temperature. This crystal belongs to a centric triclinic space group, and the chromophore and crown ether alternate to form a magnetically diluted vanadyl system. The EPR study has revealed the rhombic spin Hamiltonian parameters $g_z = 1.952(1)$, $g_x = 1.985(2)$, $g_y = 1.990(3)$, $|A_z| = 18.8(3)$, $|A_x| = 7.6(3)$ and $|A_y| > 5.5$ mT, where the z, x and y principal axes are along the V=O and nearly along the V–OH_2 and V–Cl bonds, respectively. Errors of these parameters are large, especially in A_y, owing to many broad hyperfine linewidths resulting in overlapping. A negative sign is suggested for all the principal A values. Three d–d* transitions, $d_{xy} \rightarrow d_{xz}$ (12.9 kcm^{-1}), $d_{xy} \rightarrow d_{yz}$ (15.2) and $d_{xy} \rightarrow d_{x^2-y^2}$ (17.0), and a charge-transfer transition, a_1(related to $d_{x^2-y^2}$) $\rightarrow a_2(d_{xy})$ (27–28 kcm^{-1}) from the acetone solution, were assigned. The *trans*-$[VOCl_2(H_2O)_2]$ species is not dissociated in acetone and 2-propanol solution, but the chloro ligands are substituted with aqua ligands when there is a lot of water in the solution.

Keywords: Spectroscopic studies; Vanadium complexes; Oxo complexes; Chloride complexes; Aqua complexes

1. Introduction

Recently we have studied the X-ray crystal structures of adducts of *trans*-diaquadichlorooxovanadium(IV), *trans*-$[VOCl_2(H_2O)_2]$, with 1,4,7,10,13-pentaoxacyclopentadecane (15-crown-5; abbr. 15C5) and 5,6,8,9,11,12,14,15-octahydro-2,3-benzo-1,4,7,10,13-pentaoxacyclopentadec-2-ene (benzo-15-crown-5; B15C5) [1]. The X-ray crystallographic study of the adduct with 1,4,7,10,13,16-hexaoxacyclooctadecane (18-crown-6; abbr. 18C6) was first carried out by Jin et al. [2] and its disordered structure has been re-refined by us [1]. The structure of these adducts is clearly polymeric with hydrogen bonding where the chromophore and crown ether alternate along the polymer axis. In Fig. 1 is shown the molecular coordinate system adopted herein for the *trans*-$[VOCl_2(H_2O)_2]$ chromophore. The molecular packing in the triclinic $P\bar{1}$ unit cell of $a = 7.660(2)$, $b = 7.768(1)$, $c = 10.255(1)$ Å, $\alpha = 100.74(1)$, $\beta = 106.98(2)$, $\gamma = 100.16(2)°$ and $Z = 1$ is shown in Fig. 2, where one of the positionally disordered chromophores is drawn. The chromophore not drawn is at the reflected position of the drawn chromophore. Note that the vanadium atom is very close to the crystallographic center of symmetry. The respective hydrogen atoms in one aqua ligand are hydrogen bonded to a crystalline water molecule and the oxygen atom in the upper 18C6, and this water is also hydrogen bonded to two crown oxygen atoms in the same crown. The hydrogen bonding scheme between another aqua ligand and the lower 18C6 is the same as that given above, and so the crystal

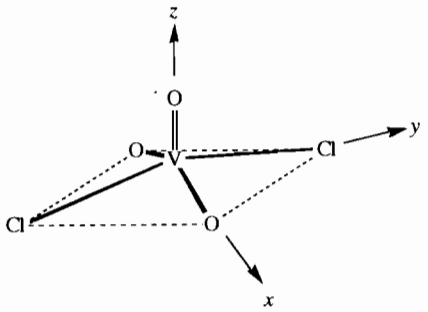

Fig. 1. The structure of the *trans*-$[VOCl_2(H_2O)_2]$ chromophore and the molecular (or principal) coordinate system adopted herein.

*Corresponding author.

SSDI 0020-1693(94)04138-L

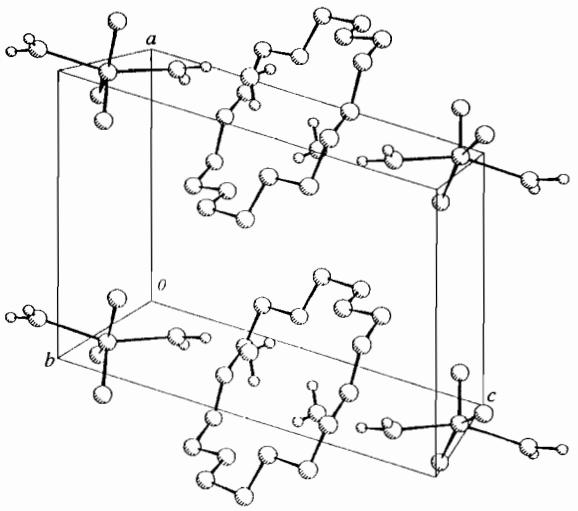

Fig. 2. The molecular packing in the *trans*-$[VOCl_2(H_2O)_2]$-(18C6)·$2H_2O$ crystal. The hydrogen atoms in the crown ether are omitted for clarity.

forms *trans*-$[VOCl_2(H_2O)_2](18C6)\cdot 2H_2O$. Because the shortest $V^{4+}\cdots V^{4+}$ distance is 7.7 Å, the crystal can be regarded as a diluted paramagnetic system; the crown ether is a diamagnetic diluent for the paramagnetic chromophore. In actual fact, the crystal exhibits an octet hyperfine structure with a broad linewidth in its powder EPR spectrum, which is rare among authentic crystals of paramagnetic compounds. This suggests the possibility for in situ observation of the g tensor and the hyperfine coupling tensor (A) using the single-crystal EPR technique.

The adducts of the *trans*-$[VOCl_2(H_2O)_2]$ chromophore with 15C5 and B15C5 also show an octet hyperfine structure in their powder spectra. Their crystals belong to the monoclinic $P2_1/n$ space group with $Z=4$, which should exhibit the so-called site splitting, while the crystal of *trans*-$[VOCl_2(H_2O)_2](18C6)\cdot 2H_2O$ is of triclinic $P\bar{1}$ space group without the site splitting. Therefore, we have adopted the latter adduct for the single-crystal EPR study in order to characterize this chromophore, so the expected hyperfine lines are eight at the most.

This chromophore is of C_{2v} symmetry at the paramagnetic site [1] and closely related to C_{4v} $[VO(H_2O)_5]^{2+}$ and $[VOCl_5]^{3-}$ species which have been studied by several investigators [3–7]. The energy level of $[VO(H_2O)_5]^{2+}$ has been established as $3d_{z^2} \gg 3d_{x^2-y^2} > 3d_{xz} = 3d_{yz} > 3d_{xy}$ and the excitation energies of the $d_{xy} \rightarrow d_{xz,yz}$ and $d_{xy} \rightarrow d_{x^2-y^2}$ transitions are 13.1 and 16.0 kcm^{-1}, respectively [3]. Polarized single-crystal spectra of $[VOCl_5]^{3-}$ in $K_3TlCl_6\cdot 2H_2O$ matrix revealed 15.5 ($d_{xy} \rightarrow d_{xz,yz}$) and 16.2 ($d_{xy} \rightarrow d_{x^2-y^2}$) kcm^{-1} transition energies [5]. It is interesting to compare the spectral properties of the present chromophore with those of the above two. Furthermore, knowledge about the g tensor and its orientation in the molecular coordinate system is very helpful for the assignment of the optical absorption bands. Thus, EPR and UV–Vis spectra of the *trans*-$[VOCl_2(H_2O)_2]$ chromophore have been studied.

2. Experimental

2.1. Single crystal preparation

The adduct compound *trans*-$[VOCl_2(H_2O)_2](18C6)\cdot 2H_2O$ was prepared by the procedure already published [1]. The blue single crystal of $0.5\times0.9\times1.3$ mm used for the EPR measurements was recrystallized from a 2-propanol (containing 3 wt.% water) solution after prolonged standing in a flask with a tight stopper at ambient temperature.

2.2. Measurements

The EPR spectra from the single crystal were observed at room temperature through the rotation around five axes in a plane close to the molecular xy plane in view of the peculiar limitation of the present sample. The spectra from the solutions were recorded at room temperature and 77 K. All measurements were carried out on a JEOL JES-ME-3X X-band spectrometer equipped with a 100 kHz field modulation for the first-derivative spectra. The magnetic field was calibrated by the splitting of Mn(II) in powdered MgO, which had previously been corrected by the splitting of Fremy's salt ($a^N = 1.300$ mT and $g = 2.0054$ [8]). The microwave frequency was measured with a Takeda-Riken frequency counter. The resonant-field intensities were estimated based on the spacings between the respective spectral lines and the line from the Li-TCNQ radical salt ($g = 2.0025$) taken as a secondary standard.

Electronic absorption spectra were recorded on a Hitachi 320 spectrophotometer at room temperature using several solvents. Solvents of special grade for spectral use were used as purchased. The Nujol mull method was also adopted with a paste of 0.1 mm thickness sandwiched between the quartz plates.

3. Analysis of single-crystal EPR spectra

Fig. 3 illustrates the relationship between the applied magnetic field H and the coordinate systems adopted for our instrumentation. The coordinate systems of (0-123) and (0-$\chi\psi\omega$) represent those fixed to the crystal and to a uni-axial type goniometer with a plastic top

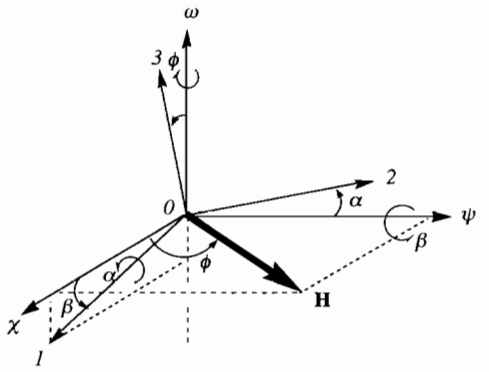

Fig. 3. The coordinate systems adopted in the EPR measurement. The crystal is mounted on the $\psi\omega$ plane, keeping the 1 axis in the $\chi\omega$ plane, and α is the semi-fixed angle between the axes ψ and 2. The magnetic field vector $\boldsymbol{H}$ is always in the $\chi\psi$ plane.

(on the quartz tube) having two faces for $\beta=0$ and 90°, respectively. By appropriate intervals in the ϕ angle, the crystal is rotated around the ω axis under the fixed α and β angles. In such a measurement, the direction of $\boldsymbol{H}$ can be represented by

$$\boldsymbol{h}=\begin{bmatrix}h_1\\h_2\\h_3\end{bmatrix}=\begin{bmatrix}\cos\beta\cos\phi\\ \sin\alpha\sin\beta\cos\phi+\cos\alpha\sin\phi\\ \cos\alpha\sin\beta\cos\phi-\sin\alpha\sin\phi\end{bmatrix} \quad (1)$$

where $\boldsymbol{h}=\boldsymbol{H}/H$ is the unit vector. The linear observation equations applicable to the least-squares procedure are expressed by the following equations

$$g_h^2=\tilde{\boldsymbol{h}}\cdot\tilde{\boldsymbol{g}}\cdot\boldsymbol{g}\cdot\boldsymbol{h}=\tilde{\boldsymbol{h}}\cdot\boldsymbol{g}^2\cdot\boldsymbol{h} \quad (2)$$

$$A_h^2=\tilde{\boldsymbol{h}}\cdot\boldsymbol{A}^2\cdot\boldsymbol{h} \quad (3)$$

$$T_h^2=\tilde{\boldsymbol{h}}\cdot\tilde{\boldsymbol{g}}\cdot\tilde{\boldsymbol{A}}\cdot\boldsymbol{A}\cdot\boldsymbol{g}\cdot\boldsymbol{h}=\tilde{\boldsymbol{h}}\cdot\tilde{\boldsymbol{T}}\cdot\boldsymbol{T}\cdot\boldsymbol{h}=\tilde{\boldsymbol{h}}\cdot\boldsymbol{T}^2\cdot\boldsymbol{h} \quad (4)$$

where the symbols are the same as Iwasaki's notation [9], and the subscript h represents that the designated squared quantity is one along $\boldsymbol{H}$.

In the preliminary measurements, a single crystal in the magnetic field was rotated around three orthogonal axes fixed to the crystal, that is, $(\alpha, \beta)=(0, 0)$, $(\pi/2, 0)$ and $(0, \pi/2)$. The majority of the observed spectra was unresolved. The remaining spectra were poorly resolved owing to the broad linewidth, which indicated that the resolution could be expected only in the region around the leading principal axis of the $\boldsymbol{A}$ tensor. Therefore, we adopted the following modified procedure for the final measurement in order to obtain as many suitable data for the analysis of the tensors as possible. The suitably oriented single crystal was fixed on a small piece of cover glass with an adhesive. A suitable orientation is the (0-123) system, close to but not the same as the molecular coordinate system. Then the piece of glass was mounted on the $\psi\omega$ plane of the goniometer with silicon grease. The α angles adopted were 0.5, 21.4, 44.9, 62.0 and 90.5° for a fixed $\beta=0°$ and ϕ interval of 5°. The relationship between the (0-123) system and the crystallographic oblique (0-*abc*) system was obtained by measuring the interfacial angles of the crystal and taking the X-ray oscillation photographs around the two crystallographic axes.

The angular dependence of the average field of m $(=m_I)=\pm5/2$ resonance lines and that of the difference between the $\pm5/2$ resonance fields were fitted to the $\boldsymbol{g}^2$ and $\boldsymbol{T}^2$ tensors by means of the conventional linear least-squares procedure. The data for the three selected α angles were used in the least-squares. The $\boldsymbol{A}$ tensor was obtained from the partition of the $\boldsymbol{T}$ tensor with the $\boldsymbol{g}$ tensor. Then, they were refined by the least-squares procedure for the non-linear observation function in which all eight hyperfine resonant fields of all the data for the five α angles were used in each cycle of the refinement. The partial derivatives were calculated by the following type of equation: $\partial H/\partial g_{ij}\approx 100\Delta H/\sigma(g_{ij})$ where $\sigma(g_{ij})$ was the standard deviation of the ij element of each tensor.

In the non-linear least-squares refinement, we used Eq. (6) as the observation function for the resonant field strength of $m_I=\pm m$ transition ($H(\pm m)$) derived from a more general formalism by Iwasaki [9], and the quadrupolar term ($\boldsymbol{P}$) was assumed to be zero in view of the broader linewidth against the splittings between the resonance lines. For the same reasons, the weight of $w=\tan\theta/\tan 80°$ was adopted where θ was a slant angle of the first-derivative hyperfine profile

$$H(\pm m)=\frac{g_e}{2g}\left[\left(H_e\mp mK\mp\frac{2mP_m}{K}\right)+\sqrt{\left(H_e\mp mK\mp\frac{2mP_m}{K}\right)^2-\frac{A_m}{2}}\right] \quad (5)$$

or the approximately extracted form of the square root

$$H(\pm m)=\frac{g_e}{g}\left[(H_e\mp mK)-\frac{A_m}{(H_e\mp mK)}\mp\frac{2mP_m}{K}\right] \quad (6)$$

where g_e and H_e represent the free electron g value and the resonant field strength of g_e species, respectively, and

$$A_{7/2}=7\mathrm{Tr}\tilde{\boldsymbol{A}}\cdot\boldsymbol{A}+42(\tilde{\boldsymbol{k}}\cdot\boldsymbol{A}\cdot\tilde{\boldsymbol{A}}\cdot\boldsymbol{k})-49K^2 \quad (7a)$$

$$A_{5/2}=19\mathrm{Tr}\tilde{\boldsymbol{A}}\cdot\boldsymbol{A}+6(\tilde{\boldsymbol{k}}\cdot\boldsymbol{A}\cdot\tilde{\boldsymbol{A}}\cdot\boldsymbol{k})-25K^2 \quad (7b)$$

$$A_{3/2}=27\mathrm{Tr}\tilde{\boldsymbol{A}}\cdot\boldsymbol{A}-18(\tilde{\boldsymbol{k}}\cdot\boldsymbol{A}\cdot\tilde{\boldsymbol{A}}\cdot\boldsymbol{k})-9K^2 \quad (7c)$$

$$A_{1/2}=31\mathrm{Tr}\tilde{\boldsymbol{A}}\cdot\boldsymbol{A}-30(\tilde{\boldsymbol{k}}\cdot\boldsymbol{A}\cdot\tilde{\boldsymbol{A}}\cdot\boldsymbol{k})-K^2 \quad (7d)$$

$$P_{7/2}=3\mathrm{Tr}\tilde{\boldsymbol{P}}\cdot\boldsymbol{P}+30(\tilde{\boldsymbol{k}}\cdot\boldsymbol{P}\cdot\tilde{\boldsymbol{P}}\cdot\boldsymbol{k})-69(\tilde{\boldsymbol{k}}\cdot\boldsymbol{P}\cdot\boldsymbol{k})^2/2 \quad (7e)$$

$$P_{5/2}=9\mathrm{Tr}\tilde{\boldsymbol{P}}\cdot\boldsymbol{P}-30(\tilde{\boldsymbol{k}}\cdot\boldsymbol{P}\cdot\tilde{\boldsymbol{P}}\cdot\boldsymbol{k})+33(\tilde{\boldsymbol{k}}\cdot\boldsymbol{P}\cdot\boldsymbol{k})^2/2 \quad (7f)$$

$$P_{3/2}=13\mathrm{Tr}\tilde{\boldsymbol{P}}\cdot\boldsymbol{P}-70(\tilde{\boldsymbol{k}}\cdot\boldsymbol{P}\cdot\tilde{\boldsymbol{P}}\cdot\boldsymbol{k})+101(\tilde{\boldsymbol{k}}\cdot\boldsymbol{P}\cdot\boldsymbol{k})^2/2 \quad (7g)$$

$$P_{1/2}=15\mathrm{Tr}\tilde{\boldsymbol{P}}\cdot\boldsymbol{P}-90(\tilde{\boldsymbol{k}}\cdot\boldsymbol{P}\cdot\tilde{\boldsymbol{P}}\cdot\boldsymbol{k})+135(\tilde{\boldsymbol{k}}\cdot\boldsymbol{P}\cdot\boldsymbol{k})^2/2 \quad (7h)$$

$$K^2=\tilde{\boldsymbol{h}}\cdot\tilde{\boldsymbol{g}}\cdot\tilde{\boldsymbol{A}}\cdot\boldsymbol{A}\cdot\boldsymbol{g}\cdot\boldsymbol{h}/g^2 \quad (7i)$$

$$\boldsymbol{k}=\boldsymbol{A}\cdot\boldsymbol{g}\cdot\boldsymbol{h}/gK \quad (7j)$$

$$H_e=h\nu/g_e\beta \quad (7k)$$

and the other symbols are as given in Ref. [9]. The principal values were obtained by the diagonalization of the tensors refined thus and their standard deviations were also computed from the diagonal elements of the variance matrices. All computations were carried out at the Data Processing Center of Ehime University by using Fortran programs coded for general purposes in single-crystal EPR by one of the present authors (N.A.).

4. Results and discussion

Shown in Fig. 4 are the typical EPR spectra observed for the single crystal of *trans*-$[VOCl_2(H_2O)_2]$-(18C6)·$2H_2O$. The hyperfine structure from an isolated V^{4+} ion should be an octet with uniform intensity. However, the spectrum (A), which is one of those that exhibit the most resolved hyperfine structure, shows a strange octet; the nearly uniform spaced lines have two resonance intensities. The lines at the far sides always have a larger intensity than those between them, as seen from the spectra in (A) and (B). This irregularity in intensity is peculiar to the first-derivative EPR spectrum arising from the poorly resolved hyperfine structure due to a broad linewidth. The second-derivative spectra from our instrumentation were of too small an intensity to analyze more precisely. Integration of these spectra should give a trapezoidal outline with a wavy top as a whole. Dipolar broadening widths of 10–15 mT are expected based on the dipolar summation. The poorly resolved first-derivative spectra give rise to systematic errors, such as those arising from the obscure reflection

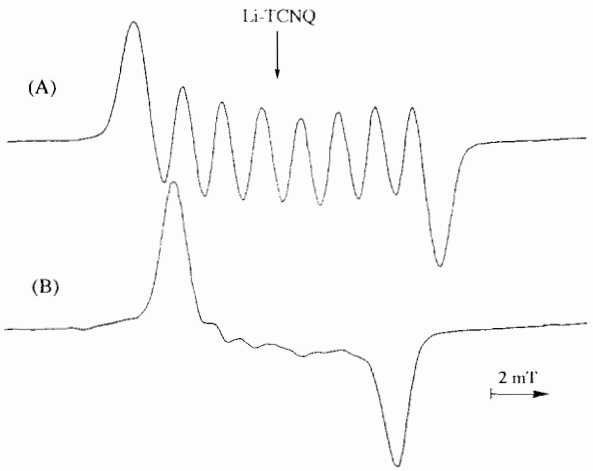

Fig. 4. Typical first-derivative EPR spectra observed for the single crystal of *trans*-$[VOCl_2(H_2O)_2](18C6)\cdot 2H_2O$. The applied magnetic fields in (A) and (B) are nearly parallel and perpendicular to the V=O bond.

point of each line (presuming that it is at the middle point between the top and bottom peaks) and from the data deficiency, in addition to large accidental errors in the resonant-field data due to the small slant angles of the spectral lines. If spectral simulation (a second-order correction could be necessary in the vanadyl system) were carried out for all the spectra, the systematic errors would be decreased to some extent.

The ϕ angular dependence of the hyperfine resonant fields is shown in Figs. 5 and 6. The refined principal values of the $\boldsymbol{g}$ and $\boldsymbol{A}$ tensors are summarized in Table 1. The principal coordinate system of the $\boldsymbol{A}$ tensor seemed to be rotated around the z axis (common to the $\boldsymbol{A}$ and $\boldsymbol{g}$ tensors within 3°) from that of the $\boldsymbol{g}$ tensor by about 20° at first sight; indeed the above method does not presuppose a common coordinate system for the $\boldsymbol{g}$ and $\boldsymbol{A}$ tensors. Therefore, we have examined the standard deviations for the unitary matrices, $\boldsymbol{u}$: the maximum was 0.28. Extremely large deviations occur in the u_{23} and u_{32} elements, since no datum has been

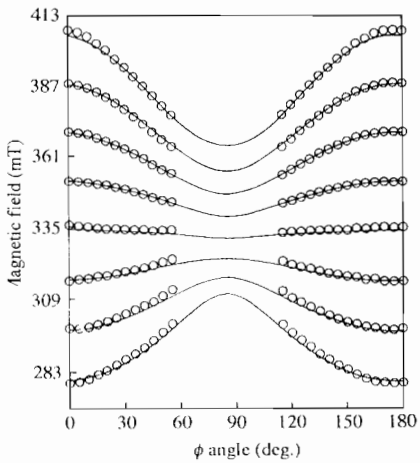

Fig. 5. The ϕ angular dependence of the EPR spectra for the *trans*-$[VOCl_2(H_2O)_2]$ chromophore at $\alpha=0.5°$. The open circles are the observed data and the solid lines show the non-linear least-squares curve fitting to the resonant field by the $\boldsymbol{g}$ and $\boldsymbol{A}$ tensors.

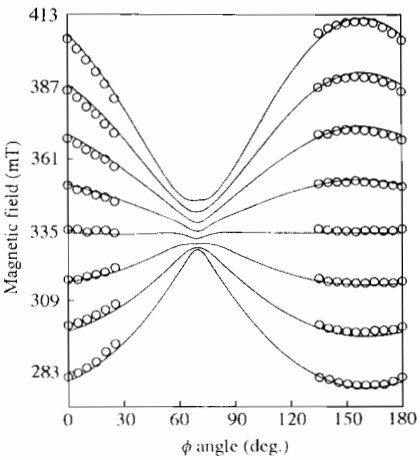

Fig. 6. The ϕ angular dependence of the EPR spectra for the *trans*-$[VOCl_2(H_2O)_2]$ chromophore at $\alpha=90.5°$.

Table 1
The principal values of the g and A tensors observed for the *trans*-$[VOCl_2(H_2O)_2]$ chromophore together with their e.s.d.s in parentheses[a]

Principal values (e.s.d.)		Direction of axis
$g_z = 1.952(1)$	$\|A_z\| = 18.8(3)$ mT	along V=O bond
$g_x = 1.985(2)$	$\|A_x\| = 7.6(3)$ mT	nearly along V–OH_2 bond
$g_y = 1.990(3)$	$\|A_y\| = 2.6(7)$ mT	nearly along V–Cl bond
$\langle g \rangle = 1.975$	$\langle A \rangle = 9.7$ mT	

[a]The systematic errors due to unresolved hyperfine structure and others are disregarded. The signs for A values are probably all negative. We are inclined to propose $A_y \approx 6$ mT in place of 2.6 mT, which gives $\langle A \rangle = 10.8$ mT (see text).

observed in the wide range around the 2 and 3 axes, especially wide around the 3 axis, as seen from the same Figs. The angular uncertainty corresponding to the largest $\sigma(\boldsymbol{u})$ is about 15°, so that mutual rotation between the principal coordinate systems cannot be presumed. A common principal coordinate system to the g and A tensors sounds more reasonable for the present chromophore with an ordinary square-pyramidal geometry. The z axes of the g and A tensors which are actually in good accord with each other correspond to the direction in which the best and most data have been obtained.

The principal z, x and y axes are nearly parallel to the 1, 2 and 3 axes, respectively, as can be seen from Figs. 5 and 6. Accordingly, the standard deviations are in the ascending order of the $z<x<y$ principal values. The systematic error may also be large in the y values. A trial and error simulation procedure (excluding the second-order correction) for the powder sample gave tolerable results when the following parameters were used: $g_z = 1.952$, $g_x = 1.984$, $g_y = 1.990$, $A_z = 18.8$ mT, $A_x = 7.6$, $A_y > 5.5$, $\Delta H_z = 13$, $\Delta H_x = 11$, $\Delta H_y = 10$ mT. The powder spectrum has two sharper lines at both the neighbouring sides of $g = 1.990$ with a separation of about 14 mT between them. These lines are deformed with a too small A_y valuc, by which the above threshold is obtained. The threshold is close to the value of $2.6 + 3\sigma(A_y)$. Therefore, we are inclined to propose the A_y value to be about 6 mT in place of 2.6 mT.

The isotropic hyperfine coupling constants in the present solutions, A_{iso}, are 10.8–11.0 mT which is consistent with $\langle A \rangle = (18.8 + 7.6 + 6)/3 = 10.8$ mT, showing little solvent dependence. On the other hand, the principal A_{zz} value for the electron–nuclear dipolar interaction should be of opposite sign to the A_{xx} and A_{yy} values, because $(A_{zz}, A_{xx}, A_{yy}) = (-4P/7, 2P/7, 2P/7)$ for the d_{xy} singly occupied system in a strongly applied field, where $P = g\beta g_N \beta_N / \langle r^3 \rangle$ with r being the separation of the d electron from the nucleus [10]. The sign of P is positive for vanadium in view of the positive nuclear magnetic moment of this atom. Therefore, the signs of the principal A and A_{iso} values are all negative.

The *trans*-$[VOCl_2(H_2O)_2]$ chromophore can have a finely approximated C_{2v} local symmetry at the V^{4+} site [1]. The X-ray crystallographical H_2O–V–OH_2 and Cl–V–Cl angles in the present crystal are 152 and 150°, respectively. This crystal shows orientational disorder at the chromophore site, to which the centric space group with $Z = 1$ is attributed. On the other hand, the same angles in the 15C5 adduct are 153.2 and 142.7°, and in the B15C5 adduct they are 153.8 and 144.8°. Therefore, the Cl–V–Cl angle is sensitive to the environment. Taking into account that these bond angles are different from 180° and the limit of the above angular errors, the principal coordinate systems of the tensors are in accord with the molecular coordinate system shown in Fig. 1.

Since the $3d_{xy}$ ground-state Kramers doublet has been established for the $[VO(H_2O)_5]^{2+}$ and $[VOCl_5]^{3-}$ species, as mentioned in Section 1, the same ground-state doublet can be taken for the *trans*-$[VOCl_2(H_2O)_2]$ chromophore in the following discussion. This ground-state doublet is quite consistent with the fact that the chromophore does not show superhyperfine splitting due to the chloro ligands in any solvent.

Within the framework of the simple crystal field theory (SCFT), the anisotropic g components for the d_{xy} ground-state doublet in a C_{2v} symmetric field are given by [11]

$$g_z = 2 - 8\lambda/\Delta E_{x^2-y^2} \quad (8a)$$

$$g_x = 2 - 2\lambda/\Delta E_{xz} \quad (8b)$$

$$g_y = 2 - 2\lambda/\Delta E_{yz} \quad (8c)$$

where ΔE is the energy separation between the d_{xy} and designated level and λ is the spin–orbit coupling constant of 160–100 cm^{-1} [12,13]. Therefore, all g components should be less than g_e and the g_z value should be the smallest of the three. The observed g_y is larger than g_x by $1.6\sigma(g)$, which may be of only slight statistical significance. Nevertheless, the C_{2v} symmetry of the paramagnetic site will be proved by the spectral evidence. The rhombicity in the g tensor indicates that the $3d_{yz}$ level is higher than the $3d_{xz}$ level. From Eqs. (8) and the observed g values, the ratios of $\Delta E_{yz}/\Delta E_{xz}$, $\Delta E_{yz}/\Delta E_{x^2-y^2}$ and $\Delta E_{xz}/\Delta E_{x^2-y^2}$ are calculated to be 1.4, 1.0 and 0.73, respectively. The indicated level sequence is $3d_{x^2-y^2} \approx 3d_{yz} > 3d_{xz} > 3d_{xy}$.

The estimated g_z and A_z values of 1.952 and 18.8 mT ($= 0.0176$ cm^{-1}) are closer to those of $[VOCl_5]^{3-}$, 1.9450 and 0.0173 cm^{-1} [6], than those of $[VO(H_2O)_5]^{2+}$, 1.9331 and 0.0183 cm^{-1} [4], which suggests that the equatorial crystal field is similar to that of the $[VOCl_5]^{3-}$ species, that is, the separation between the $3d_{x^2-y^2}$ and $3d_{xy}$ levels is enlarged by substitution of the two aqua ligands with the two chloro ligands.

The molecular orbital (MO) theory is indispensable for treating the electronic structure of vanadyl com-

plexes. The electron donation from the p_z orbitals of the chloro ligands to the $3d_{yz}$ orbital, which makes a π-bond with the p_y orbital of the oxo ligand, may elevate the b_2* level from that with no π-donation. The aqua ligand has only a small π-donating ability in comparison with the chloro ligand. Therefore, the $3d_{yz}$ (b_2*) > $3d_{xz}$ (b_1*) sequence is possible. The V=O (formal double bond), V–OH_2 and V–Cl bond distances are 1.57, 2.00 and 2.31 Å, respectively [1, 2]. These bond distances indicate strong π-bonds between the vanadium and oxo oxygen atom, which suggests the antibonding $3d_{z^2}$ (a_1*) level is much higher than the non-bonding $3d_{xy}$ (a_2) level, probably >40 kcm^{-1}; therefore the $3d_{z^2}$ (a_1*) level will not appear in the following discussion. It is interesting to know the energy sequence of the bonding a_1 (centered on basal σ orbitals rather than the $d_{x^2-y^2}$ orbital), b_1 and b_2 orbitals, because in $[VO(H_2O)_5]^{2+}$ the bonding e_π (associated with $d_{xz,yz}$) level is higher than the a_1 ($d_{x^2-y^2}$) level [3], while a reverse sequence has been suggested for $[VOCl_5]^{3-}$ [7].

The optical absorption spectrum observed in acetone solution was resolved into its Gaussian components by means of the SP program [14], as shown in Fig. 7(A). The fit of the composite spectra to all the observed spectra was monitored graphically ($\Delta\epsilon \leqslant 1$). In 2-propanol the same spectrum as in acetone solution was observed in the energy region lower than 22 kcm^{-1}, but a rather different spectrum appeared in the higher energy region, especially when the solution contained a substantial amount of water. There are absorption bands at 12.9 (ϵ=17), 15.2 (30), and 17.0 (6) kcm^{-1}, which can be observed at 13.5, 15.9 and 19.0 kcm^{-1} by the Nujol mull method, as shown in Fig. 8. These can be assigned to the $d_{xy} \rightarrow d_{xz}$, $d_{xy} \rightarrow d_{yz}$ and $d_{xy} \rightarrow d_{x^2-y^2}$ transitions, respectively, in view of the above EPR results. The smallest ϵ value of the 17 kcm^{-1} band is reasonable for the orbitally forbidden transition (but vibronically allowed), while the other two are orbitally allowed on the symmetry backgrounds. The width of this band is twice as broad as that of the others, which is well consistent with the above assignment, because, in MO theory, since the $d_{x^2-y^2}$ orbital in SCFT is in a linear combination with the symmetry-adapted orbital of the four basal σ orbitals of the weakly coordinated ligands, this MO level (a_1*) fluctuates with the vibration of the ligands in the basal plane [15]. The vibronic transition from the non-bonding a_2 ($3d_{xy}$) to the a_1* ($d_{x^2-y^2}$) level is possible by borrowing the transition intensity from an allowed transition of $^2A_2[(a_1)^2(a_2)^1] \rightarrow {}^2A_2[(a_1)^1(a_2)^1(a_1^*)^1]$, because the in-plane deformation vibration mixes the σ orbitals belonging to a_1 into the d_{xy} orbital; the vibration of the monodentate ligands is easy. The same reason holds for the 27–28 kcm^{-1} (27.5 kcm^{-1} by the Nujol mull method) band which may be ascribed to the transition from the bonding a_1 to the non-bonding a_2 ($3d_{xy}$) level; this transition thus has a great deal of charge-transfer (CT) character. The relatively low extinction coefficient of this CT transition may be acceptable, because the $^2A_2[(a_1)^2(a_2)^1] \rightarrow {}^2A_1[(a_1)^1(a_2)^2]$ transition is forbidden on symmetry grounds. This assignment shows the a_1 level (related to $d_{x^2-y^2}$) to be higher than the b_1 and b_2 (d_{xz} and d_{yz}) levels, which is the reverse of that for $[VO(H_2O)_5]^{2+}$. This result is consistent with the fact that, as mentioned below, the chloro ligands are dissociative or of easy substitution and that the atomic energy level (associated with the valence state ionization energy) of the chloro ligand, σ(Cl), is higher than that of the aqua ligand, $\sigma(OH_2)$.

The above assignment for the *trans*-$[VOCl_2(H_2O)_2]$ species in acetone solution is supported by the addition of water to this solution. The ϵ ratio of the 13 to 15

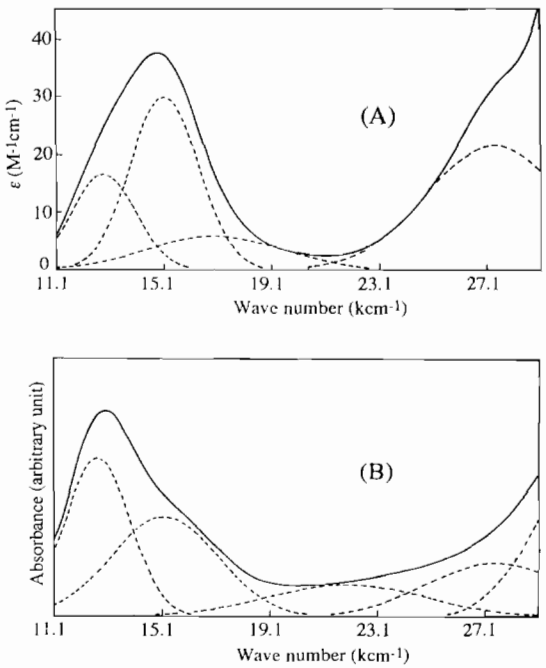

Fig. 7. Optical absorption spectra of the *trans*-$[VOCl_2(H_2O)_2]$ chromophore observed for (A) the acetone solution and (B) the water/acetone = 1/2 mixed solution. The broken lines are the Gaussian components.

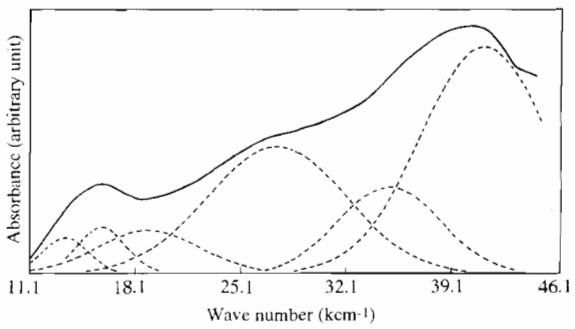

Fig. 8. Optical absorption spectrum of the *trans*-$[VOCl_2(H_2O)_2]$ chromophore observed by the Nujol mull method. The broken lines are the Gaussian components.

kcm^{-1} band changes as the amount of water increases. The spectrum observed in the water/acetone = 1/2 mixed solution appears in Fig. 7(B). The 12.7 and 15.2 kcm^{-1} bands agree with the 13 and 16 kcm^{-1} bands observed for C_{4v} $[VO(H_2O)_5]^{2+}$ [3]. Moreover, the fact that the ϵ value of the 16 kcm^{-1} band is smaller than that of the 13 kcm^{-1} band agrees well with the result observed for $[VO(H_2O)_5]^{2+}$. In the C_{4v} species, the 16 kcm^{-1} band has been ascribed to the orbitally forbidden $d_{xy} \rightarrow d_{x^2-y^2}$ transition. In the present sample the 15 kcm^{-1} band associated with the $3d_{x^2-y^2}$ orbital is also broader than the 13 kcm^{-1} band. Therefore, the *trans*-$[VOCl_2(H_2O)_2]$ species is dissolved in acetone and 2-propanol in the form of *trans*-$[VOCl_2(H_2O)_2]$, but the chloro ligands are substituted by water molecules when the solvent contains substantial water.

Acknowledgement

We thank Emeritus Professor Kazuhiko Ishizu of Ehime University for valuable discussion and encouragement.

References

[1] N. Azuma, T. Ozawa and K. Ishizu, *Polyhedron, 13* (1994) 1715.
[2] X. Jin, Z. Pan, M. Shao, D. Huang, Z. Tai and J. Zhang, *Kexue Tongbao, 29* (1984) 319.
[3] C.J. Ballhausen and H.B. Gray, *Inorg. Chem., 1* (1962) 111.
[4] R.H. Borcherts and C. Kikuchi, *J. Chem. Phys., 40* (1964) 2270.
[5] R.A.D. Wentworth and T.S. Piper, *J. Chem. Phys., 41* (1964) 3884.
[6] K. DeArmond, B.B. Garrett and H.S. Gutowsky, *J. Chem. Phys., 42* (1965) 1019.
[7] H. Kon and N.E. Sharpless, *J. Phys. Chem., 70* (1966) 105.
[8] G.E. Pake, J. Townsend and S.I. Weisman, *Phys. Rev., 85* (1952) 682.
[9] M. Iwasaki, *J. Magn. Reson., 16* (1974) 417.
[10] B.G. Goodman and J.B. Raynor, *Adv. Inorg. Chem. Radiochem., 13* (1970) 135.
[11] B.J. Hathaway and D.E. Billing, *Coord. Chem. Rev., 5* (1970) 143.
[12] T.M. Dunn, *Trans. Faraday Soc., 57* (1961) 1441.
[13] N.M. Atherton and C.J. Winscon, *Inorg. Chem., 12* (1973) 383.
[14] (a) H. Miyata and S. Tokuda, *Shokubai (Catalyst), 30* (1988) 311; (b) H. Miyata, K. Fujii, S. Inui and Y. Kubokawa, *Appl. Spectrosc., 40* (1986) 1177; (c) H. Miyata, *Chem. Express., 2* (1987) 643.
[15] N. Azuma, Y. Kohno, F. Nemoto, Y. Kajikawa, K. Ishizu, T. Takakuwa, S. Tsuboyama, K. Tsuboyama, K. Kobayashi and T. Sakurai, *Inorg. Chim. Acta, 215* (1994) 109.